Long-Term Temporal Convolutions for Action Recognition

Gül Varol, Ivan Laptev, and Cordelia Schmid, *Fellow, IEEE*

Abstract—Typical human actions last several seconds and exhibit characteristic spatio-temporal structure. Recent methods attempt to capture this structure and learn action representations with convolutional neural networks. Such representations, however, are typically learned at the level of a few video frames failing to model actions at their full temporal extent. In this work we learn video representations using neural networks with long-term temporal convolutions (LTC). We demonstrate that LTC-CNN models with increased temporal extents improve the accuracy of action recognition. We also study the impact of different low-level representations, such as raw values of video pixels and optical flow vector fields and demonstrate the importance of high-quality optical flow estimation for learning accurate action models. We report state-of-the-art results on two challenging benchmarks for human action recognition UCF101 (92.7%) and HMDB51 (67.2%).

Index Terms—Action recognition, video analysis, representation learning, spatio-temporal convolutions, neural networks

1 Introduction

Human actions and events can be seen as spatio-temporal objects. Such a view finds support both in psychology [1] and in computer vision approaches to action recognition in video [2], [3], [4], [5]. Successful methods for action recognition, indeed, share similar techniques with object recognition and represent actions by statistical models of local video descriptors. Differently to objects, however, actions are characterized by the temporal evolution of appearance governed by motion. Consistent with this fact, motion-based video descriptors such as HOF and MBH [2], [5] as well as recent CNN-based motion representations [6] have shown most gains for action recognition in practice.

The recent rise of convolutional neural networks (CNNs) convincingly demonstrates the power of learning visual representations [7]. Equipped with large-scale training datasets [8], [9], CNNs have quickly taken over the majority of still-image recognition tasks such as object, scene and face recognition [9], [10], [11]. Extensions of CNNs to action recognition in video have been proposed in several recent works [6], [12], [13]. Such methods, however, currently show only moderate improvements over earlier methods using hand-crafted video features [5].

Current CNN methods for action recognition often extend CNN architectures for static images [7] and learn action representations for short video intervals ranging from 1 to 16 frames [6], [12], [13]. Yet, typical human actions such as hand-shaking and drinking, as well as cycles of repetitive actions such as walking and swimming often last several seconds and span tens or hundreds of video frames. As illustrated in Figs. 1a and 1c actions often contain characteristic patterns with specific spatial as well as *long-term* temporal structure. Breaking this structure into short clips (see Figs. 1b and 1d) and aggregating video-level information by the simple average of clip scores [6], [13] or more sophisticated schemes such as LSTMs [14] is likely to be suboptimal.

In this work, we investigate the learning of long-term video representations. We consider space-time convolutional neural networks [13], [15], [16] and study architectures with Long-term Temporal Convolutions (LTC), see Fig. 2. To keep the complexity of networks tractable, we increase the temporal extent of representations at the cost of decreased spatial resolution. We also study the impact of different low-level representations, such as raw values of video pixels and optical flow vector fields. Our experiments confirm the advantage of motion-based representations and highlight the importance of good quality motion estimation for learning efficient representations for human action recognition. We report state-of-the-art performance on two recent and challenging human action benchmarks: UCF101 and HMDB51.

The contributions of this work are twofold. We demonstrate *(i)* the advantages of long-term temporal convolutions and *(ii)* the importance of high-quality optical flow estimation for learning accurate video representations for human action recognition. In the remaining part of the paper we discuss related work in Section 2, describe space-time CNN architectures in Section 3 and present an extensive experimental study of our method in Section 4. Our implementation and pre-trained CNN models (compatible with Torch) are available on the project web page [17].

2 Related Work

Action recognition in the last decade has been dominated by local video features [2], [4], [5] aggregated with Bag-of-Features histograms [18] or Fisher Vector representations [19]. While typical pipelines resemble earlier methods for object recognition, the use of local motion features, in particular Motion Boundary Histograms [5], has been found important for action recognition in practice. Explicit representations of the temporal structure of actions have rarely beed used with some exceptions such as the recent work [20].

Learning visual representations with CNNs [7], [21] has shown clear advantages over "hand-crafted" features for many recognition tasks in static images [9], [10], [11]. Extensions of CNN representations to action recognition in video have been proposed in several recent works [6], [12], [13], [14], [15], [16], [22], [23], [24], [25]. Some of these methods encode single video frames with static CNN features [6], [12], [14]. Extensions to short video clips where video frames are treated as multi-channel inputs to 2D CNNs have also been investigated in [6], [12], [23], [25].

Learning CNN representations for action recognition has been addressed for raw pixel inputs and for pre-computed optical flow features. Consistent with previous results obtained with hand-crafted representations, motion-based CNNs typically outperform CNN representations learned for RGB inputs [6], [23]. In this work we investigate multi-resolution representations of motion and appearance where for motion-based CNNs we demonstrate the importance of high-quality optical flow estimation. Similar findings have been recently confirmed by [26], where the authors transfer knowledge from high quality optical flow algorithms to motion vector encoding representation.

Most of the current CNN methods use architectures with 2D convolutions, enabling shift-invariant representations in the image plane. Meanwhile, the invariance to translations in time is also important for action recognition since the beginning and the end of actions is unknown in general. CNNs with 3D spatio-temporal convolutions address this issue and provide a natural extension of 2D

• G. Varol and I. Laptev are with Inria, WILLOW project-team, Département d'Informatique de l'École Normale Supérieure, ENS/Inria/CNRS UMR 8548, Paris, France. E-mail: {gul.varol, ivan.laptev}@inria.fr.
• C. Schmid is with Inria, Thoth project-team, Inria Grenoble Rhône-Alpes, Laboratoire Jean Kuntzmann, France. E-mail: cordelia.schmid@inria.fr.

Manuscript received 10 Aug. 2016; revised 22 Apr. 2017; accepted 10 May 2017. Date of publication 5 June 2017; date of current version 14 May 2018.
(Corresponding author: Gül Varol.)
Recommended for acceptance by G. Mori.
For information on obtaining reprints of this article, please send e-mail to: reprints@ieee.org, and reference the Digital Object Identifier below.
Digital Object Identifier no. 10.1109/TPAMI.2017.2712608

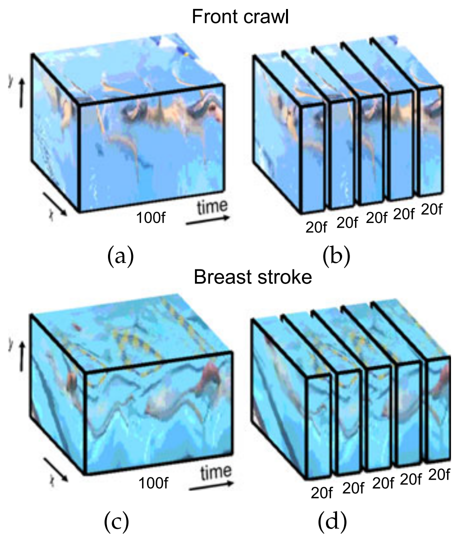

Fig. 1. Video patches for two classes of swimming actions. (a),(c): Actions often contain characteristic, class-specific space-time patterns that last for several seconds. (b),(d): Splitting videos into short temporal intervals is likely to destroy such patterns making recognition more difficult. Our neural network with Long-term Temporal Convolutions (LTC) learns video representations over extended periods of time.

CNNs to video. 3D CNNs have been investigated for action recognition in [12], [13], [15], [16]. All of these methods, however, learn video representations for RGB input. Moreover, they typically consider very short video intervals, for example, 16-frame video clips are used in [13] and 2, 7, 15 frames in [16], [15], [12] respectively. In this work we extend 3D CNNs to significantly longer temporal convolutions that enable action representation at their full temporal scale. We also explore the impact of optical flow input. Both of these extensions show clear advantages in our experimental comparison to previous methods.

3 Long-Term Temporal Convolutions

In this section we first present the network architecture. We then specify the different inputs to networks used in this work. We finally provide details on learning and testing procedures.

3.1 Network Architecture

Our network architecture with long-term temporal convolutions is illustrated in Fig. 2. The network has 5 space-time convolutional layers with 64, 128, 256, 256 and 256 filter response maps, followed by 3 fully connected layers of sizes 2048, 2048 and the number of classes. Following [13] we use $3 \times 3 \times 3$ space-time filters for all convolutional layers. Each convolutional layer is followed by a rectified linear unit (ReLU) and a space-time max pooling layer. Max pooling filters are of size $2 \times 2 \times 2$ except in the first layer, where it is $2 \times 2 \times 1$. The size of convolution output is kept constant by padding 1 pixel in all three dimensions. Filter stride for all dimensions is 1 for convolution and 2 for pooling operations. We use dropout for the first two fully connected layers. Fully connected layers are followed by ReLU layers. Softmax layer at the end of the network outputs class scores.

3.2 Network Input

To investigate the impact of long-term temporal convolutions, we here study network inputs with different temporal extents. We depart from the recent C3D work [13] and first compare inputs of 16 frames (16f) and 60 frames (60f). We then systematically analyze implications of the increased temporal and spatial resolutions for input signals in terms of motion and appearance. For the 16-frame network we crop input patches of size $112 \times 112 \times 16$ from videos with spatial resolution 171×128 pixels. We choose this baseline architecture to enable direct comparison with [13]. For the 60-frames networks we decrease spatial resolution to preserve network complexity and use input patches of size $58 \times 58 \times 60$ randomly cropped from videos rescaled to 89×67 spatial resolution.

As illustrated in Fig. 2, the temporal resolution in our 60f network corresponds to 60, 30, 15, 7 and 3 frames for each of the five convolutional layers. In comparison, the temporal resolution of the 16f network is reduced more drastically to 16, 8, 4, 2 and 1 frame at each convolutional layer. We believe that preserving the temporal resolution at higher convolutional layers should enable learning more complex temporal patterns. The space-time resolution for the outputs of the fifth convolutional layers is $3 \times 3 \times 1$ and $1 \times 1 \times 3$ for the 16f and 60f networks respectively. The two networks have a similar number of parameters in the *fc6* layer and the same number of parameters in all other layers. For a systematic study of networks with different input resolutions we also evaluate the effect of increased temporal resolution $t \in \{20, 40, 60, 80, 100\}$ and varying spatial resolution of $\{58 \times 58, 71 \times 71\}$ pixels.

In addition to the input size, we experiment with different types of input modalities. First, as in [13], we use raw RGB values from video frames as input. To explicitly learn motion representations, we also use flow fields in x and y directions as input to our networks. Flow is computed for original videos. To maintain correct flow values for network inputs with reduced spatial resolution, the magnitude of the flow is scaled by the factor of spatial subsampling. In other words, if a point moves 2 pixels in a 320×240 video frame, its motion will be 1 pixel when the frame is resized to 160×120 resolution. Moreover, to center the input data, we follow [6] and subtract the mean flow vector for each frame.

To investigate the dependency of action recognition on the quality of motion estimation, we experiment with three types of flow inputs obtained either directly from the video encoding, referred to as MPEG flow [27], or from two optical flow estimators, namely Farneback [28] and Brox [29]. Fig. 3 shows results for the three flow algorithms. MPEG flow is a fast substitute for optical flow which

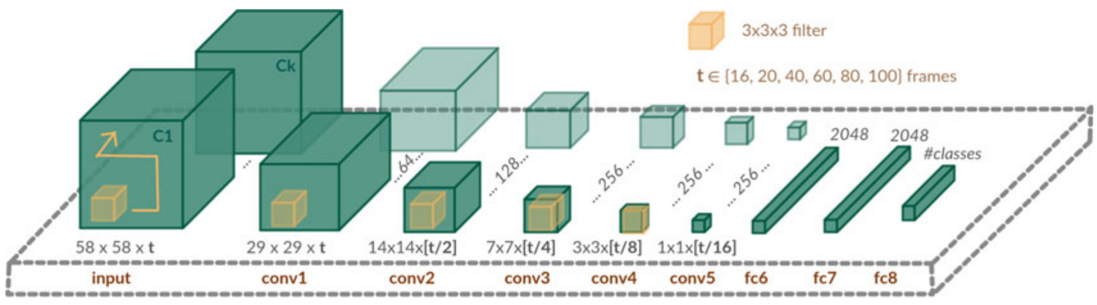

Fig. 2. Network architecture. Spatio-temporal convolutions with 3x3x3 filters are applied in the first 5 layers of the network. Max pooling and ReLU are applied in between all convolutional layers. Network input channels $C1 \ldots Ck$ are defined for different temporal resolutions $t \in \{20, 40, 60, 80, 100\}$ and either two-channel motion (*flow-x*, *flow-y*) or three-channel appearance (*R*,*G*,*B*). The spatio-temporal resolution of convolution layers decreases with the pooling operations.

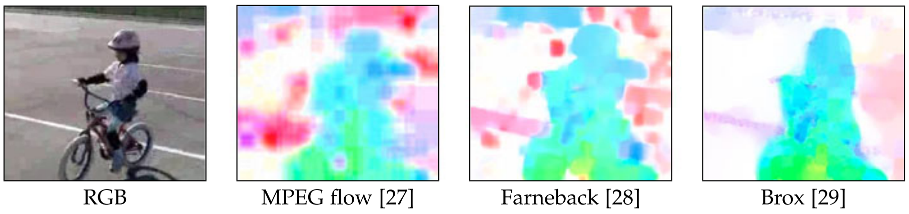

Input	Clip	Video
RGB	57.0	59.9
MPEG flow	58.5	63.8
Farneback	66.3	71.3
Brox	**74.8**	**79.6**

Fig. 3. Illustration of the three optical flow methods and comparison of corresponding recognition performance. From left to right: Original image, MPEG, Farneback and Brox optical flow. The color coding indicates the orientation of the flow. The table on the right presents accuracy of action recognition in UCF101 (split 1) for different inputs. Results are obtained with 60f networks and training from scratch (see text for more details).

we obtain from the original video encoding. Such flow, however, has low spatial resolution. It also misses flow vectors at some frames (I-frames) which we interpolate from neighboring frames. Farneback flow is also relatively fast and obtains rather noisy flow estimates. The approach of Brox flow is the most sophisticated of the three and is known to perform well in various flow estimation benchmarks.

3.3 Learning

We train our networks on the training set of each split independently for both UCF101 and HMDB51 datasets, which contain 9.5K and 3.7K videos, respectively. We use stochastic gradient descent applied to mini-batches with negative log likelihood criterion. For 16f networks we use a mini-batch size of 30 video clips. We reduce the batch size to 15 video clips for 60f networks, and 10 clips for 100f networks due to limitations of our GPUs. The initial learning rate for networks learned from scratch is 3×10^{-3} and 3×10^{-4} for networks fine-tuned from pre-trained models. For UCF101, the learning rate is decreased twice with a factor of 10^{-1}. For 16f networks, the first decrease is after 80K iterations and the second one after 45K additional iterations. The optimization is completed after 20K more iterations. Convergence is faster for HMDB51, so the learning rate is decreased once after 60K iterations and completed after 10K more iterations. These numbers are doubled for 60f networks and tripled for 100f networks, since their batch sizes are twice and three times smaller compared to 16f nets. The above schedule is used together with 0.9 dropout ratio. Our experimental setups with 0.5 dropout ratio have less iterations due to faster convergence. The momentum is set to 0.9 and weight decay is initialized with 5×10^{-3} and reduced by a factor of 10^{-1} at every decrease of the learning rate.

Inspired by the random spatial cropping during training, we apply the corresponding augmentation to the temporal dimension as in [6], which we call *random clipping*. During training, given an input video, we randomly select a point (x, y, t) to sample a video clip of fixed size. A common alternative is to preprocess the data by using a sliding window approach to have pre-segmented clips of fixed size; however, this approach limits the amount of data when the windows are not overlapped as in [13]. Another data augmentation method that we evaluate is to have a multiscale cropping similar to [23]. For this, we randomly select a coefficient for width and height separately from (1.0, 0.875, 0.75, 0.66) and resize the cropped region to the size of the network input. Finally, we horizontally flip the input with 50% probability.

At test time, a video is divided into t-frame clips with a temporal stride of 4 frames. Each clip is further tested with 10 crops, namely the 4 corners and the center, together with their horizontal flips. The video score is obtained by averaging over clip scores and crop scores. If the number of frames in a video is less than the clip size, we pad the input by repeating the last frames to fill the missing volume.

4 Experiments

We perform experiments on two widely used and challenging benchmarks for action recognition: UCF101 and HMDB51 (Section 4.1). We first examine the effect of network parameters (Section 4.2). We then compare to the state-of-the-art (Section 4.3) and present a visual analysis of the spatio-temporal filters (Section 4.4). Finally we report runtime analysis (Section 4.5).

4.1 Datasets and Evaluation Metrics

UCF101 [30] is a widely-used benchmark for action recognition with 13K clips from YouTube videos lasting 7 seconds on average. The total number of frames is 2.4 M distributed among 101 categories. The videos have spatial resolution of 320×240 pixels and 25 fps frame rate.

The HMDB51 dataset [31] consists of 7K videos of 51 actions. The videos have 320×240 pixels spatial resolution and 30 fps frame rate. Although this dataset has been considered a large-scale benchmark for action recognition for the past few years, the amount of data for learning deep networks is limited.

We rely on two evaluation metrics. The first one measures per-clip accuracy, i.e. we assign each clip the class label with the maximum softmax output and measure the number of correctly assigned labels over all clips. The second metric measures video accuracy, i.e. the standard evaluation protocol. To obtain a video score we average the per-clip softmax scores and take the maximum value of this average as class label. We average over all videos to obtain video accuracy. We report our final results according to the standard evaluation protocol, which is the mean video accuracy across the three test splits. To evaluate the network parameters we use the first split.

4.2 Evaluation of LTC Network Parameters

In the following we first examine the impact of optical flow and data augmentation. We then evaluate gains provided by long-term temporal convolutions for the best flow and data augmentation techniques by comparing 16f and 60f networks. We also investigate the advantage of pre-training on one dataset (UCF101) and fine-tuning on a smaller dataset (HMDB51). Furthermore, we study the effect of systematically increased temporal resolution for flow and RGB inputs as well as the combination of networks.

4.2.1 *Optical Flow*

The impact of the flow quality on action recognition and a comparison to RGB is shown in Fig. 3 for UCF101 (split 1). The network is trained from scratch and with a 60-frame video volume as input. We first observe that even the low-quality MPEG flow outperforms RGB. The increased quality of optical flow leads to further improvements. The use of Brox flow allows nearly 20% increase in performance. The improvements are consistent when classifying individual clips and full videos. This suggests that action recognition is easier to learn from motion compared to raw pixel values. While results in Fig. 3 were obtained for 60f networks, the same holds for 16f networks (see Table 2). We also conclude that the high accuracy of optical flow estimation plays an important role for learning competitive video representations for action

TABLE 1
Data Augmentations on UCF101 (Split 1)

Method	Clip accuracy	Video accuracy
Baseline augmentation	71.6	76.5
Random clipping	74.8	79.6
Multiscale cropping	72.5	78.1
High dropout (0.9)	74.4	78.5
Combined	**76.3**	**80.5**

All results are with 60-frame Brox flow and training from scratch. All three modifications (random clipping, multiscale cropping and high dropout) give an improvement when used alone, the best performance is obtained when combined.

recognition. Given the results in Fig. 3, we choose Brox flow for all remaining experiments in this paper.

4.2.2 Data Augmentation

Table 1 demonstrates the contribution of data augmentation when training a large CNN with limited amount of data. Our baseline uses sliding window clips with 75% overlap and a dropout of 0.5 during training. We gain 3.1% with random clipping, 1.6% with multiscale cropping and 2% with higher dropout ratio. When combined, the data augmentation and a higher dropout results in a 4% gain for video classification on UCF101 split 1. High dropout, multiscale cropping and random clipping are used in the remaining experiments, unless stated otherwise.

4.2.3 Comparison of 16f and 60f Networks

Our 16-frame and 60-frame networks have similar complexity in terms of input sizes and the number of network parameters (see Section 3). Moreover, the 16-frame network resembles the C3D architecture and enables direct comparison with [13]. We therefore study the gains provided by the 60-frame inputs before analyzing performance with systematically increasing temporal resolution (from 20 to 100 frames by steps of 20) in the next paragraph.

Table 2 compares the performance of 16f and 60f networks for RGB and flow inputs as well as for different data augmentation and dropout ratios for UCF101 split 1. We observe consistent and significant improvement of long-term temporal convolutions in 60f networks for all tested setups, when measured in terms of clip and video accuracies. Our 60f architecture significantly improves for both RGB and flow-based networks. As expected, the improvement is more prominent for clips since video evaluation aggregates information over the whole video.

We repeat similar experiments for the split 1 of HMDB51 and report results in Table 3. Similar to UCF101, flow-based networks with long-term temporal convolutions lead to significant improvements over the 16f network, in terms of clip and video accuracies. Given the small size of HMDB51, we follow [6] and also fine-tune

TABLE 2
Results for Networks with Different Temporal Resolutions and Under Variation of Data Augmentation (MS: Multiscale Cropping) and Dropout (D) for UCF101 (split 1), Trained from Scratch

Input	MS	D	Test	16f	60f	gain
RGB	x	0.5	Clip	48.4	57.0	+ 8.6
			Video	51.9	59.9	+ 8.0
Flow	x	0.5	Clip	66.8	74.8	+ 8.0
			Video	77.4	79.6	+ 2.2
Flow	✓	0.9	Clip	67.1	**76.3**	+ 9.1
			Video	78.7	**80.5**	+ 1.8

Random clipping is used in all experiments. Evaluations are on individual clips and on full videos.

TABLE 3
Results for Networks with Different Temporal Resolutions for HMDB51 (Split 1) with or without Pre-Training on UCF101

Pre-training	Test	16f	60f	gain	2D CNN [6]
x	Clip	37.0	52.6	+ 15.6	
	Video	43.9	52.9	+ 9.0	46.6
✓	Clip	40.6	**56.1**	+ 15.5	
	Video	48.3	**57.1**	+ 8.8	49.0

Flow input, random clipping, multiscale cropping and 0.9 dropout are used in all setups.

networks that have been pre-trained on UCF101. As illustrated in the 2nd row of Table 3, such pre-training gives significant improvement. Moreover, our 60f flow networks significantly outperform results of the 2D CNN temporal stream ([6], Table 2) evaluated in a comparable setup, both with and without pre-training.

4.2.4 Varying Temporal and Spatial Resolutions

Given the benefits of long-term temporal convolutions above, it is interesting to study networks for increasing temporal extents and varying spatial resolutions systematically. In particular, we investigate if accuracy saturates for networks with larger temporal extents, if higher spatial resolution impacts the performance of long-term temporal convolutions and if LTC is equally beneficial for flow and RGB networks.

To study these questions, we evaluate networks with increasing temporal extent $t \in \{20, 40, 60, 80, 100\}$ and two spatial resolutions $\{58 \times 58, 71 \times 71\}$ for both RGB and flow. We also investigate combining RGB and flow by averaging their class scores. Preliminary experiments with alternative fusion techniques did not improve over such a late fusion.

Flow networks have our previous architecture as in Fig. 2, except slightly more connections in *fc6* for 71×71 resolution. For flow input, we train our networks from scratch. For RGB input, learning appears to be difficult from scratch. Even if we extend the temporal extent from 60 frames (see Table 2) to 100 frames, we obtain 68.4% on UCF101 split 1, which is still below frame-based 2D convolution methods fine-tuned from ImageNet pre-training [6]. Although longer extent boosts the performance significantly, we conclude that one needs to pre-train RGB network on larger data.

Given the large improvements provided by the pre-training of C3D RGB network on the large-scale Sports-1M dataset in [13], we use this 16-frame pre-trained network and extend it to longer temporal convolutions in 2 steps.[1] The first step is fine-tuning the 16f C3D network. A randomly initialized fully connected (*fc*) layer of size 101 (number of classes) is added at the end of the network. Only the *fc* layers are fine-tuned by freezing the convolutional layers. We start with a learning rate of 3×10^{-4} and decrease it to 3×10^{-5} after 30K iterations for 1K more iterations. In the second step, we input longer clips to the network and fine-tune all the layers. Convolutional layers are applied to longer video clips of t frames. This results in outputs from *conv5* layer with $\lfloor t/16 \rfloor$ temporal resolution. To re-cycle pre-trained *fc* layers of C3D, we max-pool *conv5* outputs over time and pass results to *fc6*. We use a subset of the *fc6* weights for inputs of lower spatial resolution. For this phase, we run for same number of iterations, but we decrease the learning rate from 3×10^{-5} to 3×10^{-6}. We keep dropout ratio 0.5 as in the pre-trained network.

Figs. 4a and 4b illustrates results of networks with varying temporal and spatial resolutions for clips and videos of UCF101, split 1. We observe significant improvements over t for LTC networks using flow (trained from scratch), RGB (with pre-training on

1. We have also tried to pre-train our flow-based networks on Sports-1M but did not obtain significant improvements.

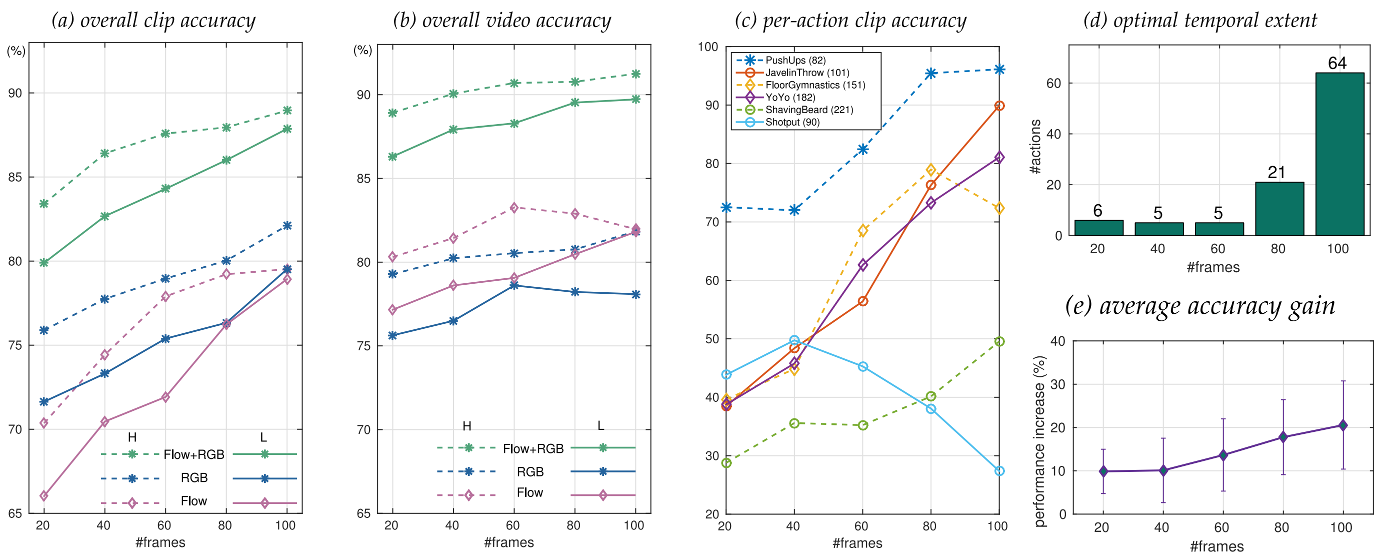

Fig. 4. Results for the split 1 of UCF101 using LTC networks of *i.* varying temporal extents t, *ii.* varying spatial resolutions [high (H), low (L)] and *iii.* different input modalities (RGB pre-trained on Sports-1M, flow trained from scratch). For faster convergence all networks were trained using 0.5 dropout and a fixed batch size of 10. Classification results are shown for clips (a) and videos (b) computed over all classes and presented for a subset of individual classes for flow input of low spatial resolution (c). The average number of frames in the training set for a class is denoted in parenthesis. (d) shows a distribution of action classes over the optimal temporal extent and (e) indicates correspondnig improvements (see text for details). With the exception of a few classes, most of the classes benefit from larger temporal extents.

Sports-1M), as well as combination of both modalities. Networks with higher spatial resolutions give better results for lower t, however, the gain of increased spatial resolution is lower for networks with long temporal extents. Given the large number of parameters in high-resolution networks, such behavior can be explained by the overfitting due to the insufficient amount of training data in UCF101. We believe that larger training sets could lead to further improvements. Moreover, flow benefits more from the averaging of clip scores than RGB. This could be an indication of static RGB information over different time intervals of the video, whereas flow is dynamic.

Fig. 4c presents results of LTC for a few action classes demonstrating a variety of accuracy patterns over different temporal extents. Out of all 101 classes, no action has monotonic decrease with the increasing temporal extent, whereas the performance of 25 action classes increased monotonically. *PushUps*, *YoYo* and *ShavingBeard* are examples of classes with high, medium and low performance that all benefit from larger temporal extents. *Shotput* is an example of a class with lower performance for longer temporal extents. A possible explanation is that samples of the *Shotput* class

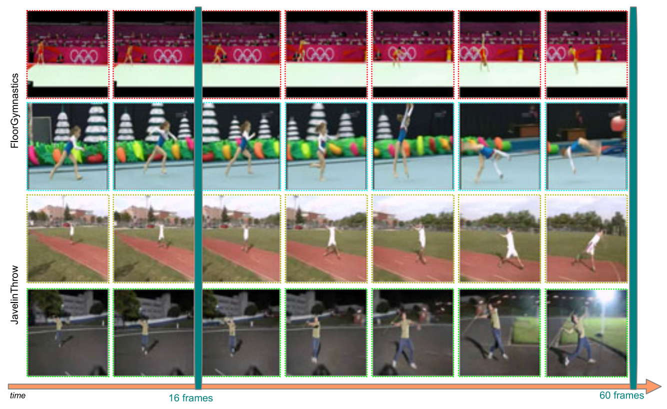

Fig. 5. The highest improvement of long-term temporal convolutions in terms of class accuracy is for *JavelinThrow*. For 16-frame network, it is mostly confused with the *FloorGymnastics* class. Here, we visualize sample videos with 7 frames extracted at every 8 frames. The intuitive explanation is that both classes start by running for a few seconds and then the actual action takes place. LTC can capture this interval, whereas 16-frame networks fail to recognize such long-term activities.

are relatively short and have 90 frames on average (we pad short clips). Two additional examples with a significant gain for larger temporal extents are *FloorGymnastics* and *JavelinThrow*, see Fig. 5 for sample frames from these two classes. We observe that both actions are composed of running followed by throwing a javelin or the actual gymnastics action. Short-term networks, thus, easily confuse the two actions, while LTC can capture such long and complex actions. For both classes, we provide snapshots at every 8th frame. It is clear that one needs to look at more than 16 frames to distinguish these actions.

Let the performance of class c for temporal extent t be $p_c(t)$. A set of classes with the maximum performance at t is then $M(t) := \{c \,|\, t \in \arg\max_{t'}(p_c(t'))\}$. Fig. 4d plots $|M(t)|$ with respect to t. The majority of classes (64 out of 101) obtain maximum performance when trained with 100f networks. To further check if there exists an "ideal temporal extent" for different actions, Fig. 4e illustrates the average performance increase $d(t)$ where;

$$d(t) := \frac{1}{|M(t)|} \sum_{M(t)} \max_{t'}(p_c(t')) - \min_{t'}(p_c(t')). \qquad (1)$$

We can observe that values of $d(t)$ are lower for shorter extents and larger for longer extents. That means actions scoring best at short extents score similar at all scales, so we cannot conclude that certain actions favor certain extents. Most actions favor long extents as the difference is largest for 100f. A possible explanation is that making the interval too long for short actions does not have much impact, whereas making the interval too short for long actions does impact the performance, see Fig. 5.

4.2.5 Combining Networks of Varying Temporal Resolutions

We evaluate combining different networks with late fusion. For final results on flow, 58×58 spatial resolution and 0.9 dropout are used for both UCF101 and HMDB51 datasets. The flow networks are learned from scratch for UCF101 and fine-tuned for HMDB51. For final results on UCF101 with RGB input, we use 71×71 spatial resolution networks fine-tuned from C3D network [13]. However, we do not further fine-tune it for HMDB51 because of overfitting, and use C3D network as a feature extractor in combination with SVM for obtaining RGB scores. Our implementation of C3D as a feature extractor and a SVM classifier achieved 80.2 and 49.7% average

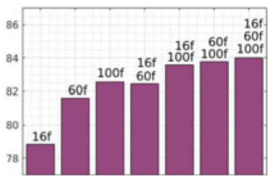

	UCF101	HMDB51
LTC$_{Flow}$ (100f)	82.6	56.7
LTC$_{Flow}$ (60f+100f)	83.8	60.5
LTC$_{RGB}$ (100f)	81.8	-
LTC$_{RGB}$ (60f+100f)	81.5	-
LTC$_{Flow+RGB}$	91.0	65.6
LTC$_{Flow+RGB}$+IDT	**91.8**	**67.7**

Fig. 6. Results for network combinations. (Left): Combination of LTC flow networks with different temporal extents on UCF101-split 1. (Right): Combination of flow and RGB networks together with IDT features on UCF101 and HMDB51-splits 1. For UCF101, flow is trained from scratch and RGB is pre-trained on Sports-1M. For HMDB51, flow is pre-trained on UCF101 and RGB scores are obtained using C3D feature extractor.

performance on 3 splits of UCF101 and HMDB51, respectively. We get similar result when fine-tuning C3D on 16-frames (80.5% on UCF101).

Fig. 6 (left) shows results for combining outputs of flow networks with different temporal extents. The combination is performed by averaging video-level class scores produced by each network. We observe that combinations of two networks with different temporal extents provides significant improvement for flow. The gains of combining more than two resolutions appear to be marginal. For final results, we report combining 60f and 100f networks for both flow and RGB, with the exception of HMDB51 RGB scores for which we use a SVM classifier on 16f feature extractor. Fig. 6 (right) shows results for combining multiscale networks of different modalities together with the IDT+FV baseline classifier [5] on split 1 of both datasets. We observe complementarity of different networks and IDT+FV where the best result is obtained by combining all classifiers.

4.3 Comparison with the-State-of-the-Art

In Table 4, we compare to the state-of-the-art on HMDB51 and UCF101 datasets. Note that the numbers do not directly match with previous tables and figures, which are reported only on first splits. Different methods are grouped together according to being hand-crafted, using only RGB or optical flow input to CNNs and combining any of these. Trajectory features perform already well, especially with higher-order encodings. CNNs on RGB perform very poor if trained from scratch, but strongly benefits from static image pre-training such as ImageNet. Recently [13] trained space-time filters from a large collection of videos; however, their method is not end-to-end, given that one has to train a SVM on top of the CNN features. Although we fine-tune LTC$_{RGB}$ based on a network learned with a short temporal span and we reduce the spatial resolution, we are able to improve by 2.2% on UCF101 (80.2 versus 82.4%) by extending the pre-trained network to 100 frames.

We observe that LTC outperforms 2D convolutions on both datasets. Moreover, LTC$_{Flow}$ outperforms LTC$_{RGB}$ despite no pre-training. Our results using LTC$_{Flow+RGB}$ with average fusion significantly outperform the Two-stream average fusion baseline [6] by 4.8 and 6.8% on UCF101 and HMDB51 datasets, respectively. Moreover, the SVM fusion baseline in [6] is still significantly below LTC$_{Flow+RGB}$. Overall, the combination of our best networks LTC$_{Flow+RGB}$ together with the IDT method[2] provides best results on both UCF101 (92.7%) and HMDB51 (67.2%) datasets. Notably both of these results outperform previously published results on these datasets, except [25] which studies best ways to combine RGB and flow streams, hence complementary to our method.

TABLE 4
Comparison with the State-of-the-Art on UCF101 and HMDB51 (Mean Accuracy Across 3 Splits)

		Method	UCF101	HMDB51
IDT	[5]	IDT+FV	85.9	57.2
	[32]	IDT+MIFS	89.1	65.1
RGB	[12]	Slow fusion (from scratch)	41.3	-
	[13]	C3D (from scratch)	44[1]	-
	[12]	Slow fusion	65.4	-
	[6]	Spatial stream	73.0	40.5
	[13]	C3D (1 net)	82.3	-
	[13]	C3D (3 nets)	85.2	-
Flow	[6]	Temporal stream	83.7	54.6
RGB + Flow	[6]	Two-stream (avg. fusion)	86.9	58.0
	[6]	Two-stream (SVM fusion)	88.0	59.4
	[33]	LSTM	88.6	-
	[22]	TDD	90.3	63.2
	[34]	Transformations	92.4	62.0
	[25]	Two-stream (conv. fusion)	**92.5**	**65.4**
+IDT	[13]	C3D+IDT	90.4	-
	[22]	TDD+IDT	91.5	65.9
	[25]	Two-str. (conv. fusion)+IDT	**93.5**	**69.2**
		LTC$_{RGB}$	82.4	-[2]
		LTC$_{Flow}$	85.2	59.0
		LTC$_{Flow+RGB}$	**91.7**	**64.8**
		LTC$_{Flow+RGB}$+IDT	**92.7**	**67.2**

[1]*This number is read from the plot in Fig. 2 [13] and is clip-based, therefore not directly comparable.*
[2]*We use C3D+SVM scores (49.7%) for HMDB51.*

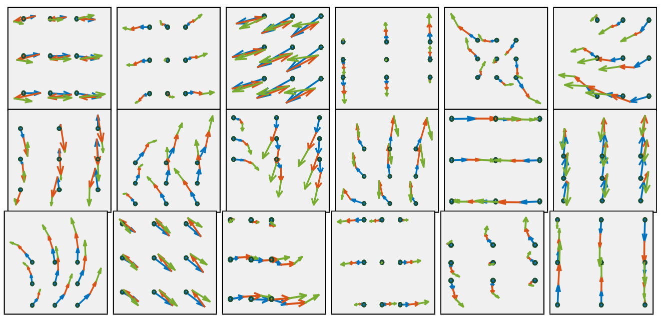

Fig. 7. Spatio-temporal filters from the first layer of the network learned with 2-channel, Brox optical flow and 60 frames on UCF101. 18 out of 64 filters are presented. Each cell in the grid represents two $3 \times 3 \times 3$ filters for 2-channel flow input (one for x and one for y). x and y intensities are converted into vectors in 2D. Third dimension (time) is denoted by putting vectors one after the other in different colors for better visualization (t = 1 blue, t = 2 red, t = 3 green). We see that LTC is able to learn complex motion patterns for video representation. Better viewed in color.

4.4 Analysis of the 3D Spatio-Temporal Filters

4.4.1 *First Layer Weights*

In order to have an intuition of what an LTC network learns, we visualize the first layer space-time convolutional filters in the vector-field form. Filters learned on 2-channel optical flow vectors have dimension $2 \times 3 \times 3 \times 3$ in terms of channels, width, height and time. For each filter, we take the two channels in each $3 \times 3 \times 3$ volume and visualize them as vectors using x- and y-components. Fig. 7 shows 18 example filters out of the 64 from a network learned on UCF101 with 60 frames flow input. Since our filters are spatio-temporal, they have a third dimension in time. We find it convenient to show them as vectors concatenated one after the other with regard to the time steps. We denote each time step with different colors and see that the filters learned by long-term temporal convolutions are able to represent complex motions in local neighborhoods, which enables to incorporate even more complex patterns in later stages of the network.

4.4.2 *High-Layer Filter Activations*

We further investigate filters from higher convolutional layers by examining their highest activations. For a given layer and a chosen

2. Our implementation of IDT+FV [5] obtained 84.5 and 57.3% for UCF101 and HMDB51, respectively.

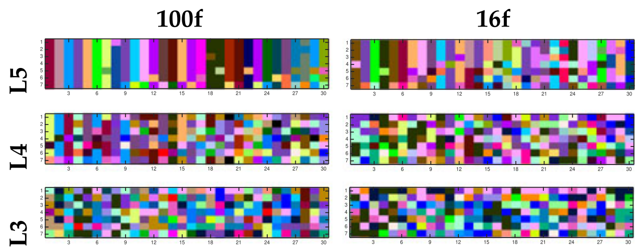

(a) Top activations of filters at *conv3-conv5* layers. Each row is another layer, indicated by L3-L5. Left is for 100 frames and right is for 16 frames networks. Colors indicate different action classes. Each color plot illustrates distribution of classes for seven top activations of 30 selected filters. Rows are maximum responding test videos and columns are filters. (best viewed in color)

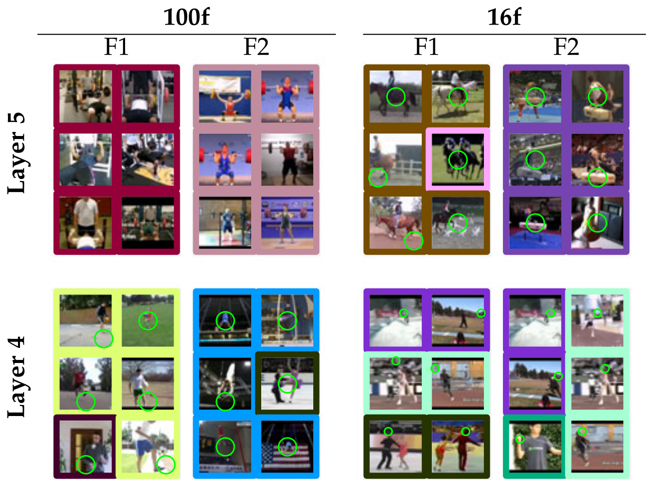

(b) Frames corresponding to videos with top activations at *conv4* and *conv5* layers. Circles indicate the spatial location of the maximum response. The visualized frames correspond to the maximum response in time.

Fig. 8. Comparison of 100f and 16f networks by looking at the top activations of filters. Better viewed in color.

filter, we record the maximum activation value for all test videos[3] for that filter. We then sort test videos according to the activation values and select the top 7 videos. This procedure is similar to [35]. We can expect that a filter should be activated by similar action classes especially at the higher network layers. Given longer video clips available to the LTC networks, we also expect better grouping of actions from the same class by filter activations of LTC. We illustrate action classes for 30 filters (x-axis) and their top 7 activations (y-axis) for the 100f and 16f networks in Fig. 8a. Each action class is represented by a unique color. The filters are sorted by their purity, i.e. the frequency of the dominating class. We assign each video the color of its ground truth class label. We see that the clustering of videos from the same class becomes more clear in higher layers in the network for both 16f and 100f networks. However, it is evident that 100f filters have more purity than 16f even in L4 and L3. Note that 16f network is trained with high resolution (112×112) flow and 100f network with low resolution (58×58) flow.

Example frames from top-scoring videos for a set of selected filters f are shown in Fig. 8b for 16f and 100f flow networks. We also provide a video on our project web page [17] to show which videos activate for these filters. We can observe that for filters f maximizing the homogeneity of returned class labels, the top activations for filters of the 100f network result in videos with similar action classes. The grouping of videos by classes is less prominent for activations of the 16f network. This result indicates that the LTC networks have higher level of abstraction at corresponding convolution layers when compared to networks with smaller temporal extents.

3. UCF101 videos are obtained by clipping different parts (*video*) from a longer video (*group*). We take one *video* per *group* assuming that *videos* from the same *group* would have similar activations and would avoid a proper analysis. In total, there are 7 test *groups* per class; therefore there can be at most 7 *videos* belonging to a class.

4.5 Runtime

Training on UCF101 takes 1.9 day for 100f (58×58) networks and 1.1 day for 16f (112×112) networks with 0.5 dropout. At test time (without flow computation), the 100f and 16f networks run at 4,452fps and 1,128fps respectively on a Titan X GPU and 8 CPU cores for parallel data loading. Although it takes more time (roughly 1.6 times) to compute one forward pass for 100f, a larger number of frames are processed per second. C3D [13] reports 313fps for a 16f network while using a larger number of parameters. Our proposed solution is therefore computationally efficient.

5 Conclusion

This paper introduces and evaluates long-term temporal convolutions and shows that they can significantly improve the performance. Using space-time convolutions over a large number of video frames, we obtain state of the art performance on two action recognition datasets UCF101 and HMDB51. We also demonstrate the impact of the optical flow quality. In the presence of limited training data, using flow improves over RGB and the quality of the flow impacts the results significantly.

Acknowledgments

This work was supported by the ERC starting grant ACTIVIA, the ERC advanced grant ALLEGRO, Google and Facebook Research Awards and the MSR-Inria joint lab.

References

[1] B. Tversky, J. Morrison, and J. Zacks, "On bodies and events," in *The Imitative Mind*, Cambridge, United Kingdom: Cambridge University Press, 2002.
[2] I. Laptev, M. Marszałek, C. Schmid, and B. Rozenfeld, "Learning realistic human actions from movies," in *Proc. IEEE Conf. Comput. Vis. Pattern Recog.*, 2008, pp. 1–8.
[3] J. C. Niebles, H. Wang, and L. Fei-Fei, "Unsupervised learning of human action categories using spatial-temporal words," *Int. J. Comput. Vis.*, vol. 79, no. 3, pp. 299–318, 2008.
[4] C. Schüldt, I. Laptev, and B. Caputo, "Recognizing human actions: A local SVM approach," in *Proc. 17th Int. Conf. Pattern Recog.*, 2004, pp. 32–36.
[5] H. Wang and C. Schmid, "Action recognition with improved trajectories," in *Proc. IEEE Conf. Comput. Vis.*, 2013, pp. 3551–3558.
[6] K. Simonyan and A. Zisserman, "Two-stream convolutional networks for action recognition in videos," in *Proc. Adv. Neural Inf. Process. Syst.*, 2014, pp. 568–576.
[7] A. Krizhevsky, I. Sutskever, and G. E. Hinton, "ImageNet classification with deep convolutional neural networks," in *Proc. Adv. Neural Inf. Process. Syst.*, 2012, pp. 1097–1105.
[8] J. Deng, W. Dong, R. Socher, L.-J. Li, K. Li, and L. Fei-Fei, "ImageNet: A large-scale hierarchical image database," in *Proc. IEEE Conf. Comput. Vis. Pattern Recog.*, 2009.
[9] B. Zhou, A. Lapedriza, J. Xiao, A. Torralba, and A. Oliva, "Learning deep features for scene recognition using places database," in *Proc. Adv. Neural Inf. Process. Syst.*, 2014, pp. 487–495.
[10] R. Girshick, J. Donahue, T. Darrell, and J. Malik, "Rich feature hierarchies for accurate object detection and semantic segmentation," in *Proc. IEEE Conf. Comput. Vis. Pattern Recog.*, 2014, pp. 580–587.
[11] Y. Taigman, M. Yang, M. Ranzato, and L. Wolf, "DeepFace: Closing the gap to human-level performance in face verification," in *Proc. IEEE Conf. Comput. Vis. Pattern Recog.*, 2014, pp. 1701–1708.
[12] A. Karpathy, G. Toderici, S. Shetty, T. Leung, R. Sukthankar, and L. Fei-Fei, "Large-scale video classification with convolutional neural networks," in *Proc. IEEE Conf. Comput. Vis. Pattern Recog.*, 2014, pp. 1725–1732.
[13] D. Tran, L. Bourdev, R. Fergus, L. Torresani, and M. Paluri, "Learning spatiotemporal features with 3D convolutional networks," in *Proc. IEEE Conf. Comput. Vis.*, 2015, pp. 4489–4497.
[14] J. Donahue, et al., "Long-term recurrent convolutional networks for visual recognition and description," in *Proc. IEEE Conf. Comput. Vis. Pattern Recog.*, 2015, pp. 2625–2634.

[15] S. Ji, W. Xu, M. Yang, and K. Yu, "3D convolutional neural networks for human action recognition," *IEEE Trans. Pattern Anal. Mach. Intell.*, vol. 35, no. 1, pp. 221–231, Jan. 2010.

[16] G. W. Taylor, R. Fergus, Y. LeCun, and C. Bregler, "Convolutional learning of spatio-temporal features," in *Proc. Eur. Conf. Comput. Vis.*, 2010, pp. 140–153.

[17] (2016). http://www.di.ens.fr/willow/research/ltc/

[18] G. Csurka, C. Dance, L. Fan, J. Willamowski, and C. Bray, "Visual categorization with bags of keypoints," in *Workshop Statist. Learn. Comput. Vis.*, 2004, pp. 1–2.

[19] F. Perronnin, J. Sánchez, and T. Mensink, "Improving the Fisher kernel for large-scale image classification," in *Proc. Eur. Conf. Comput. Vis.*, 2010, pp. 143–156.

[20] B. Fernando, E. Gavves, J. Oramas, A. Ghodrati, and T. Tuytelaars, "Modeling video evolution for action recognition," in *Proc. IEEE Conf. Comput. Vis. Pattern Recog.*, 2015, pp. 5378–5387.

[21] Y. LeCun, et al., "Backpropagation applied to handwritten zip code recognition," *Neural Comput.*, vol. 1, no. 4, pp. 541–551, 1989.

[22] L. Wang, Y. Qiao, and X. Tang, "Action recognition with trajectory-pooled deep-convolutional descriptors," in *Proc. IEEE Conf. Comput. Vis. Pattern Recog.*, 2015, pp. 4305–4314.

[23] L. Wang, Y. Xiong, Z. Wang, and Y. Qiao, "Towards good practices for very deep two-stream convnets," *CoRR*, vol. abs/1507.02159, http://arxiv.org/abs/1507.02159, 2015.

[24] H. Bilen, B. Fernando, E. Gavves, A. Vedaldi, and S. Gould, "Dynamic image networks for action recognition," in *Proc. IEEE Conf. Comput. Vis. Pattern Recog.*, 2016, pp. 3034–3042.

[25] C. Feichtenhofer, A. Pinz, and A. Zisserman, "Convolutional two-stream network fusion for video action recognition," in *Proc. IEEE Conf. Comput. Vis. Pattern Recog.*, 2016, pp. 1933–1941.

[26] B. Zhang, L. Wang, Z. Wang, Y. Qiao, and H. Wang, "Real-time action recognition with enhanced motion vector CNNs," in *Proc. IEEE Conf. Comput. Vis. Pattern Recog.*, 2016, pp. 2718–2726.

[27] V. Kantorov and I. Laptev, "Efficient feature extraction, encoding, and classification for action recognition," in *Proc. IEEE Conf. Comput. Vis. Pattern Recog.*, 2014, pp. 2593–2600.

[28] G. Farnebäck, "Two-frame motion estimation based on polynomial expansion," in *Proc. Scandinavian Conf. Image Anal.*, 2003, pp. 363–370.

[29] T. Brox, A. Bruhn, N. Papenberg, and J. Weickert, "High accuracy optical flow estimation based on a theory for warping," in *Proc. Eur. Conf. Comput. Vis.*, 2004, pp. 25–36.

[30] K. Soomro, A. Roshan Zamir, and M. Shah, "UCF101: A dataset of 101 human actions classes from videos in the wild," *CoRR*, vol. abs/1212.0402, http://arxiv.org/abs/1212.0402, 2012.

[31] H. Kuehne, H. Jhuang, E. Garrote, T. Poggio, and T. Serre, "HMDB: A large video database for human motion recognition," in *Proc. IEEE Conf. Comput. Vis.*, 2011, pp. 2556–2563.

[32] Z.-Z. Lan, M. Lin, X. Li, A. G. Hauptmann, and B. Raj, "Beyond Gaussian pyramid: Multi-skip feature stacking for action recognition," in *Proc. IEEE Conf. Comput. Vis. Pattern Recog.*, 2015, pp. 204–212.

[33] J. Y. Ng, M. J. Hausknecht, S. Vijayanarasimhan, O. Vinyals, R. Monga, and G. Toderici, "Beyond short snippets: Deep networks for video classification," in *Proc. IEEE Conf. Comput. Vis. Pattern Recog.*, 2015, pp. 4694–4702.

[34] X. Wang, A. Farhadi, and A. Gupta, "Actions ~ transformations," in *Proc. IEEE Conf. Comput. Vis. Pattern Recog.*, 2016, pp. 2658–2667.

[35] M. D. Zeiler and R. Fergus, "Visualizing and understanding convolutional networks," in *Proc. Eur. Conf. Comput. Vis.*, 2014, pp. 818–833.